Using Infrared Imaging to Evaluate Bond Uniformity in Si Structures: JPL Meso-Gyro Failure Analysis Study

Joanne Wellman, Karl Yee, – *Jet Propulsion Laboratory, Pasadena, CA*
Helen Avila – *California State University, Northridge, CA*
November 30, 2002

Introduction:

Solid-state microelectronics devices are generally built upon the unit cell of the transistor. This gives microelectronics technology a distinct advantage over MEMS devices, which have no such building block to streamline design, fabrication, reliability, or qualification tools and guidelines[1]. Advances in MEMS technology are therefore dictated by the end-user application – the need for airbag sensors, biomedical drug delivery systems, etc. – and restrictions to fundamental design are limited primarily by size, performance specifications, and the designer's imagination. This broad design potential and the fundamentally dynamic nature of most MEMS devices introduce performance degradation and failure mechanisms that do not exist in the engineering knowledge base inherited from standard microelectronics engineering. Surface-to-bulk ratio increases with decreasing feature size and at micron-level MEMS dimensions mechanical issues (stiction, wear, bond strength, etc…) become dominant and fundamental material parameters (elasticity, fracture strength, etc…) can be significantly different from traditional macroscopic systems.

MEMS, as a technology, is expanding (see Figure 1), as indicated by a growing share in the commercial MEMS market (predicted unit shipments of up to 189.4 million in 2006[2]), which necessitates the development of new tools to evaluate their performance, quality, and reliability. One common thread through current leading commercial MEMS efforts is the need for high-quality, controlled silicon bonding. Si wafer-wafer bonding issues have been identified as the "key to MEMS high-volume manufacturing.[3]" Various bonding methods are now widely used to fabricate flow channels in microfluidic applications spanning biotech, computer, medical and aerospace industries. This encompasses applications such as infusion pumps, metered dose inhalers, drug delivery systems, ink jet printers, chromatography, capillary electrophoresis systems for DNA detection systems, micropneumatics, pressurized packaging needs, and micropropulsion. Micropropulsion will play a central role in such high-visibility future NASA missions, such as interferometry, where minute attitude control maneuvers are required to accurately maintain a formation of spacecraft, or for future microspacecraft probes, weighing 10 kg or less. Highly miniaturized microfluidics sensors and lab-packages are needed for in-situ science on future Mars missions, small landers, and in the non-aerospace sector in anti-terrorism applications, for example.

Infrared imaging (IR) is commonly used to inspect Si bonds, typically in transmission mode[4,5,6]. An IR source is placed on one side of the bonded surface and a detector on the opposite side images the IR signal as heat flows through the sample and across the bond. However, transmission information is not so useful if the bond stack contains a highly reflective metal layer. We have applied non-transmission IR imaging to study quality of Au thermocompression bonds and Au/Si eutectic bonds in the Si-based JPL meso-gyro device as a non-destructive evaluation tool.

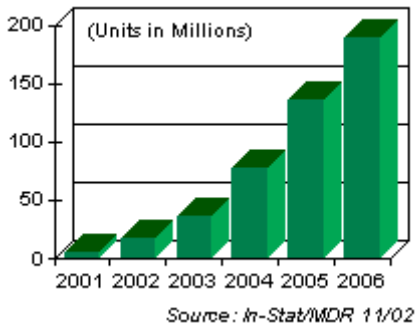

Figure 1. Worldwide forecast for MEMS in consumer electronics.[2]

Gyro Description

The JPL meso-gyro is a 2 degree of freedom, resonant, vibratory system. As observed in the laboratory frame, rotation of the device produces a coupling between the two normal modes, whereby motion along one principle axis will excite motion along the 2nd principle axis. The gyro is operated by driving it into resonance along one of its principle axes; the excitation along the orthogonal axis due to Coriolis coupling is then capacitively sensed, from which the rate of rotation is derived.

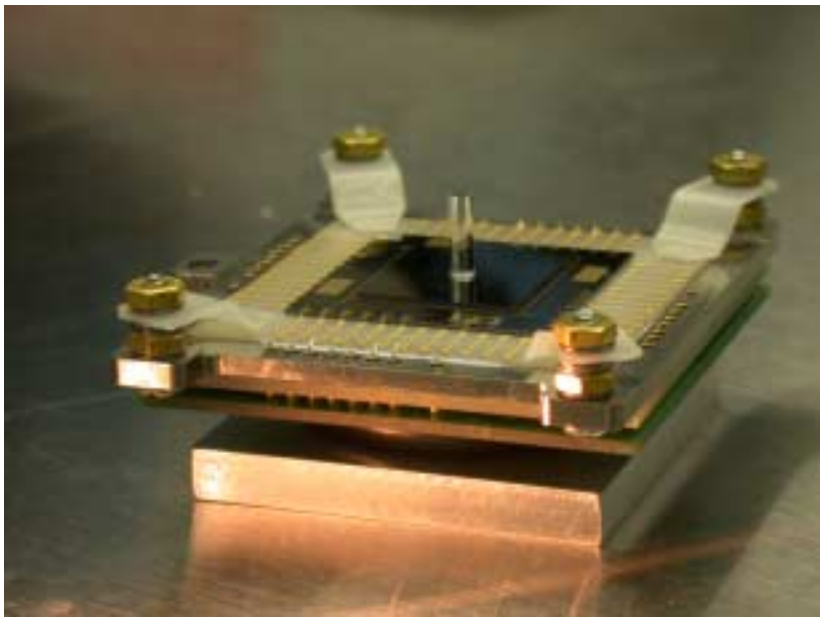

Figure 2. Gyro mounted to test fixture.

The sensor part of the meso-gyro is fabricated using standard bulk micro-machining techniques. Two silicon wafers (the resonator and the baseplate) are wet etched and plasma etched to define the geometry of the gyro. They are then metalized to form the drive and sense pads, the electrical lines and the bond pads. The resonator and base plate are then bonded together at four points, which are the only points of contact between the resonator and base plate. (This resonator/base plate bond is the interface of interest in the infrared imaging study.) Pyrex posts are then anodically bonded to the top and bottom of the resonator. The Pyrex posts are the part of the gyro that couples to the Coriolis force. The fabrication process is illustrated in Figure 3.

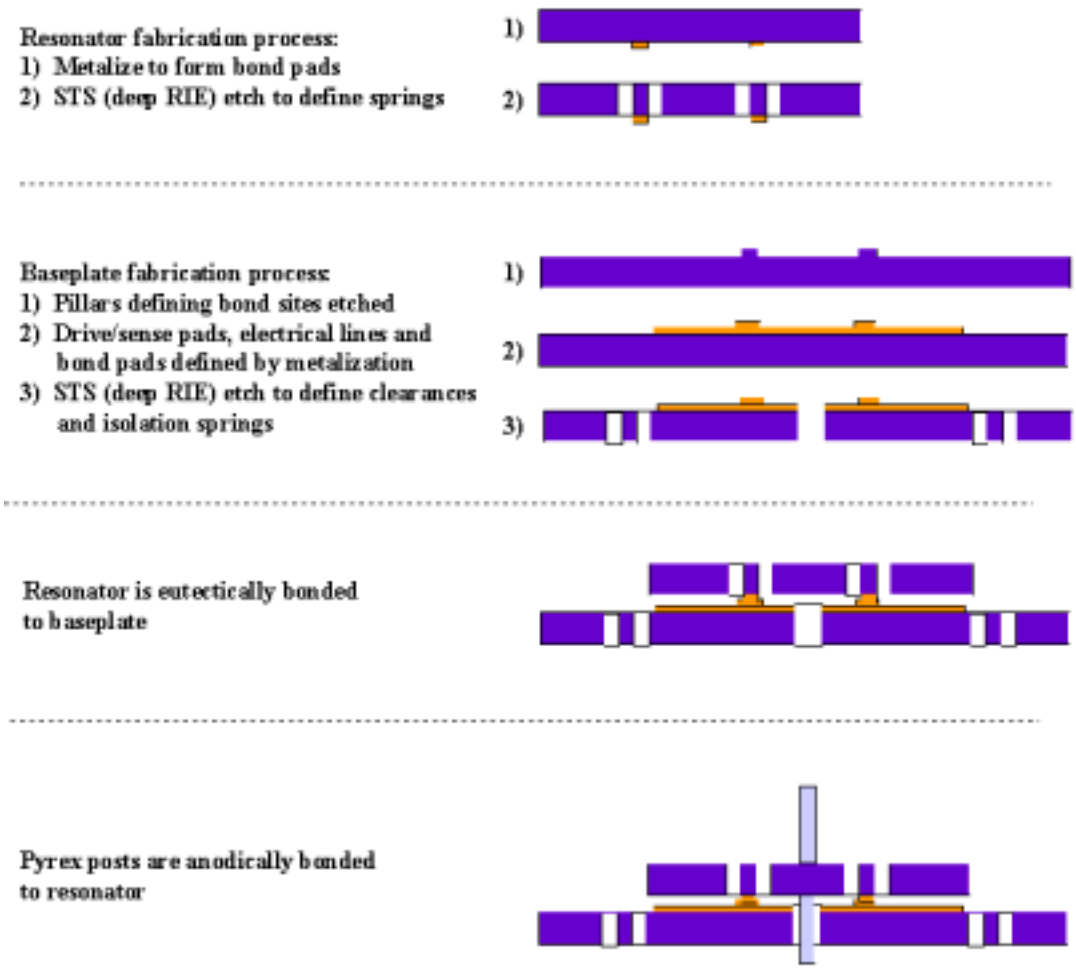

Figure 3. JPL Meso-gyro fabrication process.

The coupling between the two modes is maximized when the resonant frequencies of the two modes are identical. If the frequencies are matched, the gyro is said to be degenerate. Symmetry of construction is necessary to attain degeneracy. In particular, the bonds between the resonator and baseplate must be of near identical quality and construction. Symmetry alone is insufficient to attain a precision device. The primary source for energy losses is the resonator to baseplate bonds; each bond individually must be of high quality to ensure a long ring down time (i.e. a high "Q" factor) for the gyro. The pyrex to silicon anodic bonds are another potential source for energy losses. For these reasons, the reliability analysis of the meso-gyro was focused on the resonator/baseplate and the resonator to Pyrex post bonds.

Details of Bond Construction

The geometry of the bond sites for the resonator to baseplate bond is shown in Figure 4. The initial configuration consisted of 4 bonds, one per side; also, gold-gold thermo-compression bonds were used. Partially due to feedback from the reliability analysis, the configuration was changed to 8 bonds (two per side) and the thermocompression bond was changed to a eutectic bond. The bond geometry was chosen so that the bonds

themselves would be minimally stressed during the rocking of the gyro. The layering of materials on the baseplate was: Si, SiO_2, Ti, Pt and Au. For the resonator, we have: Si, Cr and Au. No diffusion barrier was used on the resonator in this configuration so that a Au-Silicon bond could be formed. The two wafers were bonded in vacuum, under a compressive load, at high temperature (see Figure 5).

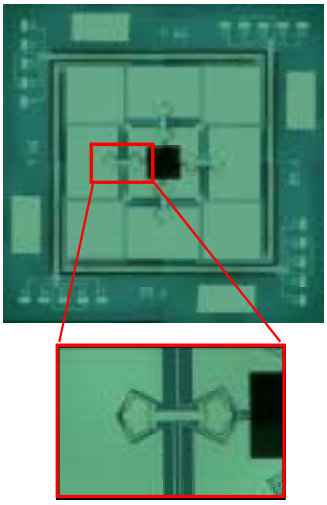

Metalization pattern of baseplate, with close-up of bond site

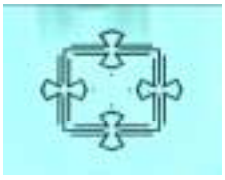

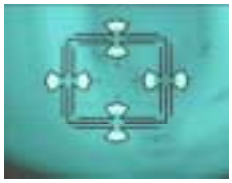

Top view and bottom view of resonator.

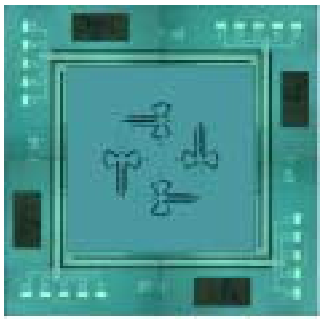

Gyro with resonator bonded to baseplate

Figure 4. Resonator/baseplate bond geometry.

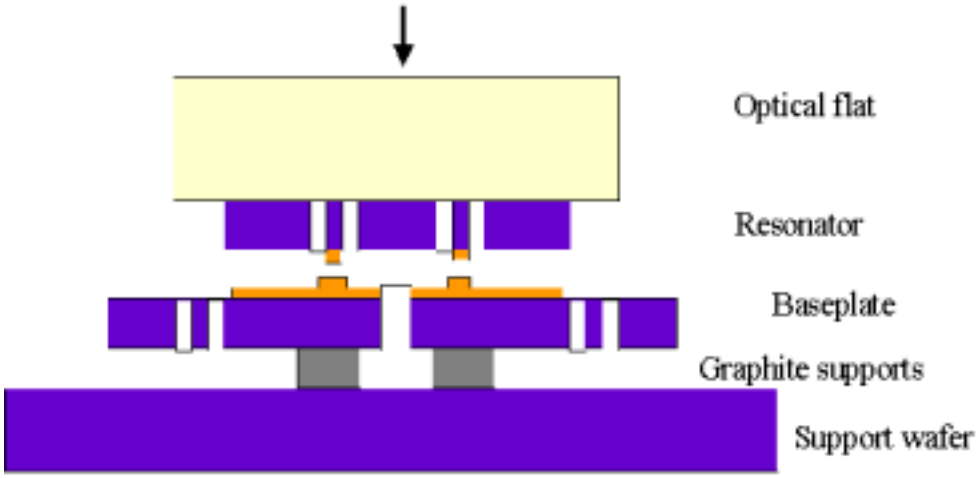

Figure 5. Resonator/baseplate bonding process

The anodic bonding of the Pyrex posts to the resonator was accomplished by heating the gyro, aligning the post to the resonator, applying a compressive load, then applying high voltage across the junction (see Figure 6).

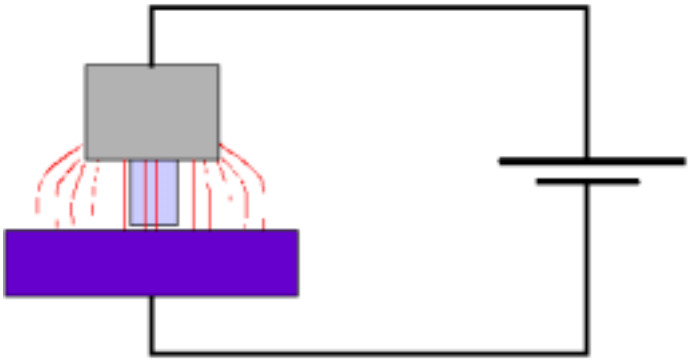

Figure 6. Si/Pyrex post anodic bonding process.

Reliability Analysis Results

Both destructive (DE) and non-destructive (NDE) evaluation was performed on gyro samples to ascertain bond quality. The goal was to correlate the results from both forms of analysis so that non-destructive analysis methodologies alone could eventually be used to ensure the quality of working devices. Methodologies employed included bond pull tests, SEM imaging, EDS analysis, and IR imaging.

Other diagnostic techniques were attempted, but did not yield meaningful results. Fine-focus x-ray analysis proved non-optimal for this device. The metal layers are too thin relative to the thickness of the silicon in this device, causing the detected signal to be dominated by the silicon. It was hoped that precision resistance measurements across the bonds could differentiate between good and bad bonds; however, this turned out not to be

the case. Acoustic microscopy was attempted on anodic bond samples. However, the technique was incapable of differentiating between good and partial bonds.

Shown below in Figure 7 are SEM micrographs of the bond sites of a typical, early design meso-gyro, where the resonator and baseplate have been pulled apart. The results clearly show that a significant fraction of the bond pad area is not successfully bonding. Complementary EDS analysis showed that the seemingly unbonded areas are primarily gold; thus, one can conclude that the bond failure occurred at the gold to gold interface between the resonator and baseplate.

Figure 7. 40x magnification SEM micrographs of the four baseplate bond pads after removal of the resonator plate

Higher magnification inspection of the bond pads revealed that the failure was due to bonding taking place only over very small, localized regions, as shown in Figure 8. These results were part of the motivation for changing the bond pad geometry, and for switching from gold to gold thermocompression bonds to Au-Si eutectic bonds.

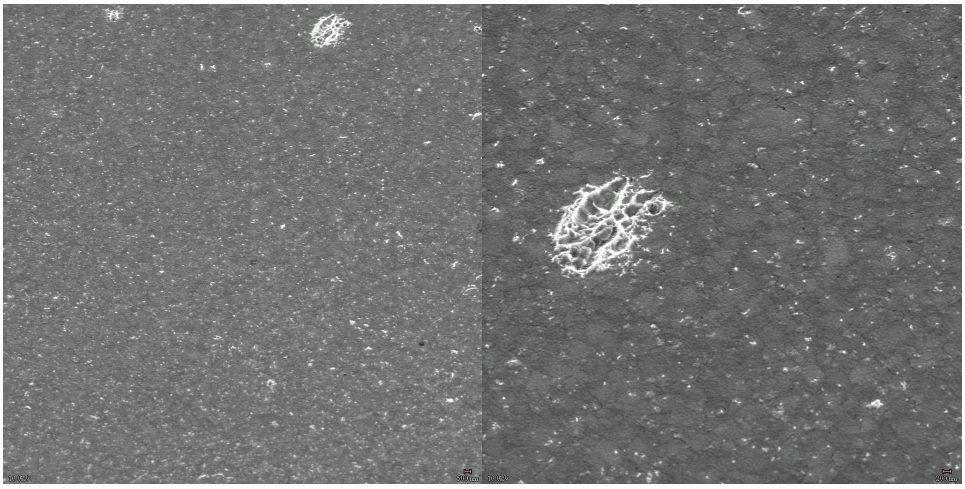

Figure 8. 3000X and 9000X magnification SEM image of Au bond metallization after destructive pull. The light-colored feature is on the order of 1.5 microns in diameter.

SEM micrograph analysis was also helpful in identifying a surface contamination problem, which hindered the anodic bonding process. Shown below (Figure 9 and Figure 10) are SEM images of sectioned anodic bonding samples. The first set was of photos are for the sample with the surface contaminant; the second set of photos are for a sample in which a new surface cleaning procedure was used.

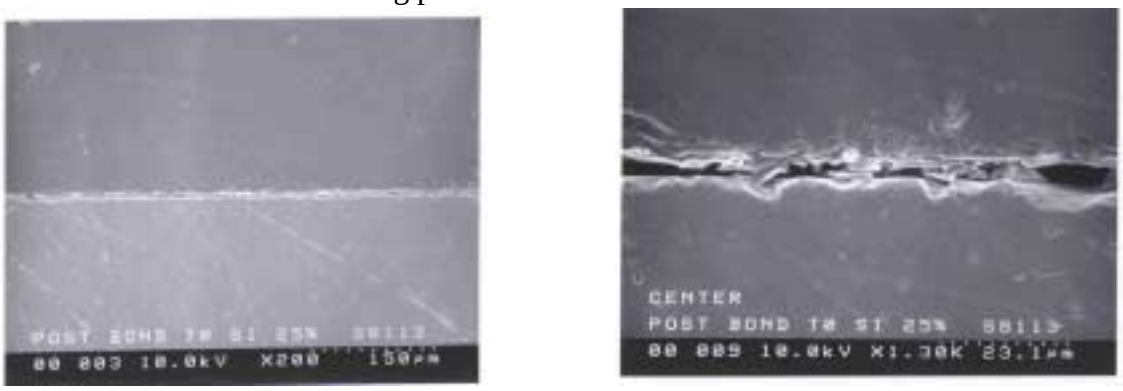

Figure 9. Cross section of anodically bonded pyrex post to silicon prior to new cleaning procedure (200x and 1300x magnification). Note existence of gap a the pyrex/silicon interface

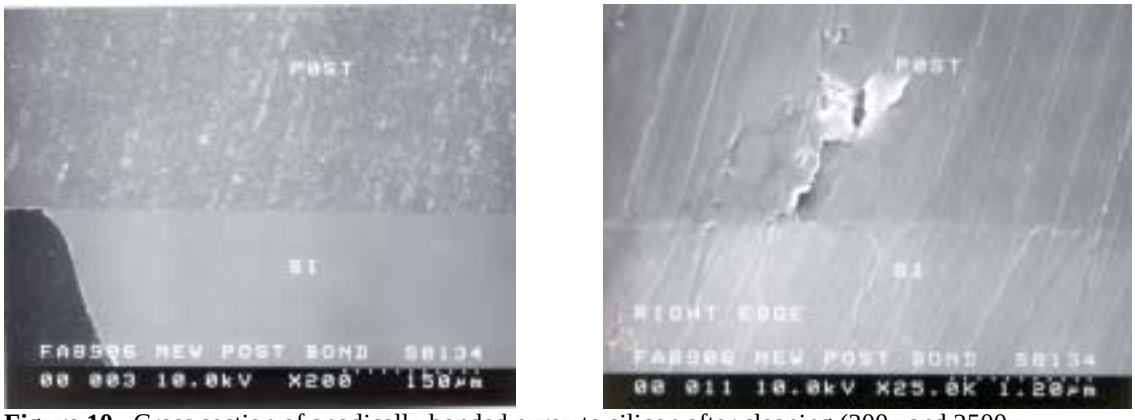

Figure 10. Cross section of anodically bonded pyrex to silicon after cleaning (200x and 2500x magnification

Infrared Imaging Results:

Silicon is transparent at infrared wavelengths, while gold is opaque in this range; thus, infrared microscopy should be a useful diagnostic for NDE of the gyro's metal bonds. The imaging system used centers on a portable infrared focal plane detector array camera, the ThermaCAM infrared imaging radiometer, manufactured by FLIR Systems™[7]. The ThermaCAM detector is a 256 × 256 platinum silicide focal plane array, with a spectral band of 3.4-5 μm. The detector operates at cryogenic temperatures, and is cooled by an internal Stirling Cycle refrigerator. Because there are no strict alignment requirements (no scanning), no portability complications of a liquid nitrogen bath,. and a long working distance (>3 cm), this IR imaging system provides a simple, clean, and flexible means of imaging the Au thermocompression bond stack interfaces.

IR imaging of several meso-gyro devices in different design stages showed interesting features in the bond pad areas. For example, in the early design Au/Au thermocompression bonded samples one can see areas of high contrast in several of the bond pads (see Figure 11). Our interpretation of this image is that these features indicate variations in the Au/Au interface, and therefore, a higher probability of non-uniform bonding across the area of the bond pad. In another case, close inspection of these contrast variations revealed that the symmetry of the IR image was broken on one bond pad: 3 of the bonds showed features on the outer radial edge while the other had features on the inside edge. This was an indication that the pressure applied during the thermocompression bonding process was non-uniform and that the carbon chuck and the gyro were not perfectly coplanar. The carbon chuck geometry was redesigned to give more uniform pressure across the bond pad, which successfully resulted in greater bond uniformity and, consequently, improved gyro performance (lower Q).

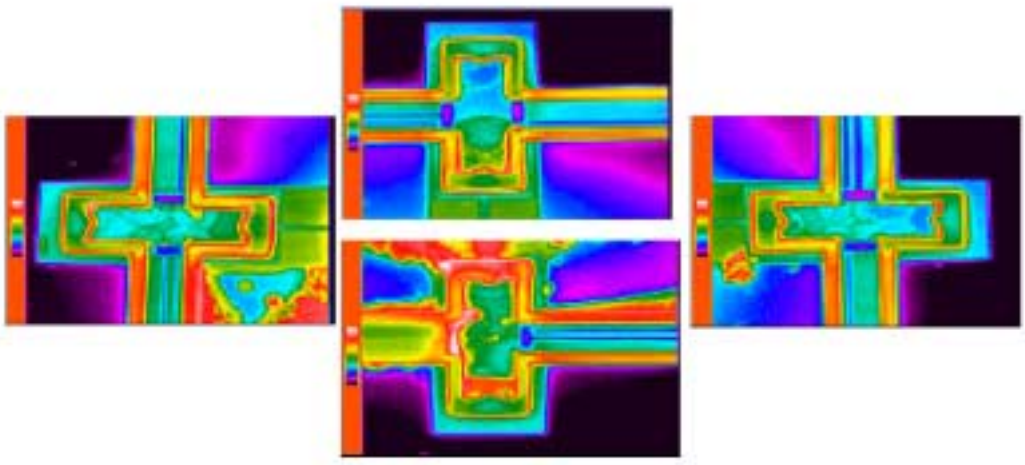

Figure 11. Infrared images of meso-gyro Au thermo-compression bond sites taken at room temperature. Because the sample is in thermal equilibrium with the surrounding environment, the apparent temperature variations must be due to emissivity and structural variations in the bond stack.

The next step was to correlate the bond pad microstructure with IR contrast. The research plan would have been a joint effort between Dr. David Via (AFRL) and JPL, with Dr. Via performing detailed cross-sectional FIB analysis at various points of a bond

that had been previously studied with IR imaging. Unfortunately, financial constraints have delayed this work indefinitely.

Initial eutectic bonding results for the meso-gyro were poor; IR imaging showed promise in revealing this. Figure 12 shows SEM micrographs of baseplate bond pads on an early eutectic bond attempt. This particular sample exhibited total bond failure (the resonator and baseplate fell apart when dicing was attempted to get access to the bond sites). The relatively smooth surfaces are indicative of material flow. EDS analysis (Figure 13) showed that the failure of the bond occurred at the SiO_2 interface of the baseplate. Figure 14 shows the IR images of the same sample before dicing was attempted. The data was taken after initially cooling the samples, then monitoring the evolution of temperature gradients as the samples were brought to room temperature. Apparent in the images is the existence of structure primarily at the periphery of the bond pads, indicative of bonding taking place only over a very small region.

Figure 12. SEM micrographs of bond pads of initial eutectic bond attempt

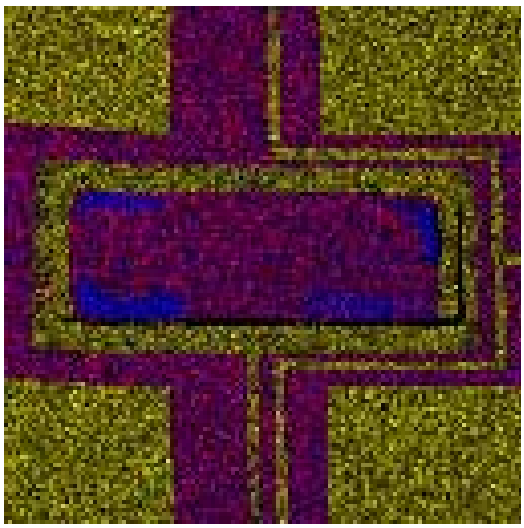

Figure 13. EDS elemental map of failed eutectic bond. Preponderance of oxygen at the surface is indicative of failure of the bond at the SiO_2 interface. Color code: Gold = Au, Blue = Si, Red = O.

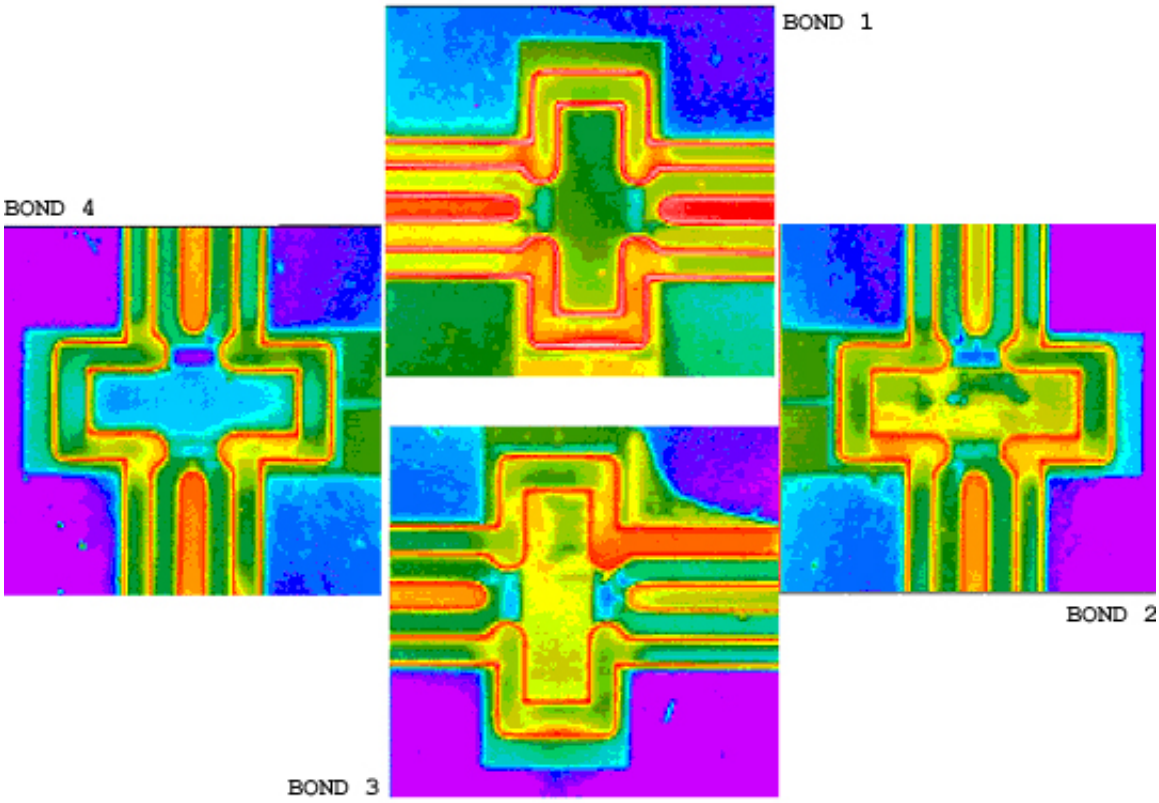

Figure 14. IR microscopy images of failed eutectic bonds. Note the absence of much of the structure seen in Figure 11. The structure seen in BOND 2 was traced back to possible contamination on the pad prior to bonding.

The problem with the IR data is that a uniform looking bond interface can either be indicative of total bond failure, or a very good bond. The two extremes are inseparable from an IR scan alone. However, IR data is useful for ascertaining a problem in situations in which incomplete uniformity exists when total uniformity is expected. An example is shown in Figure 15. Here, the corner of the gyro was inadvertently bonded during the eutectic bonding process, resulting in a dead device.

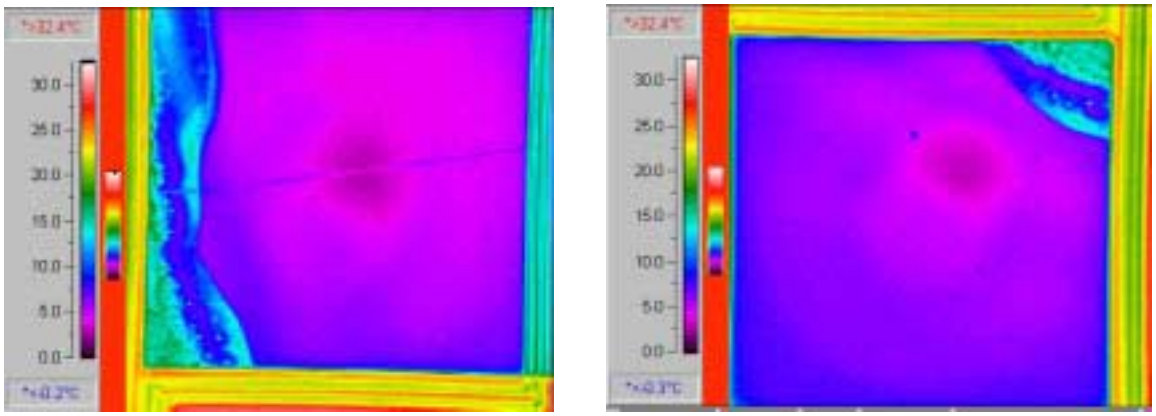

Figure 15. IR data showing bonding occurring in regions in which bonds should not exist

Conclusions:

We have used a non-transmission, room temperature IR imaging as part of the reliability study of the JPL meso-gyro to investigate bond uniformity as a test case for applying this technique to bonds in MEMS devices. Contrast in IR images appears to be a good indication of non-uniformity across the bond pad. Full correlation of IR image contrast with bond interface microstructure is the clear next step toward using IR as a known good die test for metalized bonds in Si structures.

ACKNLOWEDGEMENTS

The authors would like to acknowledge the JPL meso-gyro team (Kirill Schleglov, Ken Hayworth, Dorian Challoner, and Dean Wiberg) and Ron Ruiz of the JPL Failure Analysis Laboratory for their contributions. This work was carried out at the Jet Propulsion Laboratory, California Institute of Technology, under contract with the National Aeronautics and Space Administration, Code AE, under the NASA Electronics Parts and Packaging Program (NEPP). Additional support was provided by DARPA/SPO, NASA Code R, and CISM for meso-gyro development.

---

[1] Peter Clark, "Q&A: Bob Rao of Intel," *EE Times* (www.eetimes.com), September 17, 2002.

[2] "MEMS in Consumer Electronics Not Child's Play Anymore," In-Stat/MDR (www.instat.com) report, Novermber 13, 2002.

[3] A. R. Mirza, EV Group, A. A. Ayon, Massachusetts Institute of Technology, "Silicon Wafer Bonding,: Key to MEMS High-Volume Manufacturing", *Sensors Express* (www.sensorsmag.com), December, 1998.

[4] Schmidt, M., *Proceedings of the IEEE*, **86** (1998) p.1575.

[5] Pan CT, *et. al.*, *Journal of Micromechanics and Microengineering*, **12** (2002) p. 611-615.

[6] Plossl A, Krauter G, Materials Science & Engineering R-Report, **25** (1999) pp.1-88.

[7] http://www.flirthermography.com/cameras/application/1000/